



Full length article

# Optimization of non-linear gradient in hydrophobic interaction chromatography for the analytical characterization of antibody-drug conjugates



Balázs Bobály, Giuseppe Marco Randazzo, Serge Rudaz, Davy Guillarme, Szabolcs Fekete\*

School of Pharmaceutical Sciences, University of Geneva, University of Lausanne, CMU - Rue Michel Servet 1, 1211 Geneva 4, Switzerland

## ARTICLE INFO

## Article history:

Received 14 July 2016

Received in revised form

25 November 2016

Accepted 15 December 2016

Available online 16 December 2016

## Keywords:

Hydrophobic interaction chromatography

Antibody-drug-conjugate

Method development

Retention modelling

Non-linear gradient

## ABSTRACT

The goal of this work was to evaluate the potential of non-linear gradients in hydrophobic interaction chromatography (HIC), to improve the separation between the different homologous species (drug-to-antibody, DAR) of commercial antibody-drug conjugates (ADC). The selectivities between Brentuximab Vedotin species were measured using three different gradient profiles, namely linear, power function based and logarithmic ones. The logarithmic gradient provides the most equidistant retention distribution for the DAR species and offers the best overall separation of cysteine linked ADC in HIC. Another important advantage of the logarithmic gradient, is its peak focusing effect for the DAR0 species, which is particularly useful to improve the quantitation limit of DAR0.

Finally, the logarithmic behavior of DAR species of ADC in HIC was modelled using two different approaches, based on i) the linear solvent strength theory (LSS) and two scouting linear gradients and ii) a new derived equation and two logarithmic scouting gradients. In both cases, the retention predictions were excellent and systematically below 3% compared to the experimental values.

© 2016 Elsevier B.V. All rights reserved.

## 1. Introduction

Antibody-drug conjugates (ADCs) represent a new generation of protein biopharmaceuticals for the effective treatment of various types of cancer [1–3]. Those products show inherent heterogeneity, which has to be evaluated by the simultaneous use of a number of different analytical techniques combined with state of the art sample preparation approaches [4–10]. Hydrophobic interaction chromatography (HIC) is a unique tool for the characterization of cysteine conjugated ADCs [11–15]. These products are formed through partial reduction of the antibody's (IgG1) inter-chain disulfide bonds. The reduced cysteines are then alkylated with a preformed drug-linker. The process results in conjugates with a distributed drug load with 0, 2, 4, 6 or 8 drugs incorporated per antibody and an average drug to antibody ratio (DAR) of ~4. Since the distribution of the loaded drugs and the average DAR are critical quality attributes of ADCs, their thorough characterization is required. The main benefit of HIC – over other denaturing modes

of chromatography – is that the native Y-shape conformation of the antibody is preserved under the mild conditions, even when the disulfide bridges are reduced [15,16]. Therefore, for cysteine linked ADCs, the individual DARs can be separated in HIC on the basis of the number of attached hydrophobic drugs. Distribution of the loaded drugs and average DAR can then be determined from the peak areas.

Loaded DAR species possessing 0–8 conjugated cytotoxic drugs form an homologous series of proteins. Under linear gradient conditions, homologous series often show non-equidistant elution profiles. This behavior has already been reported for DAR species [11,13–15]. In such a case, the general linear gradient elution might suffer from poor selectivity and unnecessarily large peak spacing in the same chromatogram. Jandera reported that non-linear gradients are effective tools for selectivity tuning when separating consecutive peaks in homologous series of small molecules in reversed-phase liquid chromatography (RPLC). The study showed the efficacy of concave power function type gradients in the separation of alkylbenzenes and oligostyrenes [17]. Recently, Joshi et al. reported non-linear reversed-phase gradient separation of granulocyte colony-stimulating factor (G-CSF) and its related impurities [18]. Authors used a segmented gradient approach using non-linear gradients described by power functions. The final method

\* Corresponding author.

E-mail address: [szabolcs.fekete@unige.ch](mailto:szabolcs.fekete@unige.ch) (S. Fekete).

was described as a combination of concave and convex gradients resulting in a sigmoidal gradient profile. To find out the best chromatographic conditions and gradient shape, the method was optimized by a multistep trial and error approach. Very similar method development approach was also used for the cation-exchange separation of monoclonal antibody charge variants [19]. In another study, an algorithm was developed to generate optimized non-linear gradient functions for shotgun proteomics RP experiments to improve peak distribution of peptide peaks [20].

Here, we present a successful method development approach for the non-linear gradient HIC separation of ADC DAR species. First, the best performing logarithmic gradient profile was theoretically derived from the linear solvent strength theory (LSS). Using only two scouting linear gradients, logarithmic-like gradient elution profile (segmented multi-linear approaching) was predicted by a chromatographic modelling software. On the other hand, by applying the extended LSS model for logarithmic gradient profile, retention time prediction became feasible on the basis of two logarithmic scouting gradients. Applicability and reliability of this method development approach was evaluated by separating cysteine conjugated commercially available brentuximab vedotin payloads. The theoretically derived logarithmic gradient profile was compared to instrument built-in power-type gradient profiles. To the best of our knowledge, this is the first study describing logarithmic gradient separation for homologous series of proteins.

## 2. Experimental

### 2.1. Reagents and analytes

Water was obtained from a Milli-Q Water Purification System from Millipore (Bedford, MA, USA). Isopropyl alcohol (IPA) was ULC-MS grade and purchased from Biosolve (Valkenswaard, Netherlands). Sodium chloride (NaCl) monosodium phosphate and sodium hydroxide (NaOH) were obtained from Sigma-Aldrich (Buchs, Switzerland).

Commercial ADC (Brentuximab vedotin 5 mg/ml) was kindly provided by the Center of Immunology Pierre Fabre (Saint-Julien en Genevois, France) and injected as received.

### 2.2. Instrumentation

All the experiments were performed using a Waters Acquity UPLC™ system equipped with a binary solvent delivery pump, an autosampler and fluorescence detector (FL). This system includes a 5 mL sample loop and a 2  $\mu$ L FL flow-cell. The loop was directly connected to the injection switching valve (no needle seat capillary). The connection tube between the injector and column inlet was 0.13 mm I.D. and 250 mm long (passive preheating included), and the capillary located between the column and detector was 0.10 mm I.D. and 150 mm long. The overall extra-column volume ( $V_{ext}$ ) was about 14  $\mu$ L as measured from the injection seat of the auto-sampler to the detector cell. The measured dwell volume ( $V_d$ ) was around 100  $\mu$ L. Data acquisition and instrument control were performed by Empower Pro 3 Software (Waters).

The mobile phase pH was measured using a SevenMulti S40 pH meter (Mettler Toledo, Greifensee, Switzerland).

### 2.3. Chromatographic conditions

Mobile phase salt concentration was set on the basis of previous studies to ensure appropriate elution window for all DAR species [13,14]. Mobile phase A was 4.0 M aqueous NaCl solution containing 10 mM monosodium phosphate. After dissolving NaCl, the pH of mobile phase A was set to 7.0 by titrating with 1 M aqueous NaOH solution. For complete recovery of hydrophobic DAR

species and improved selectivity, the mobile phase B contained IPA as organic modifier. As recently reported, IPA concentration was optimized for correct average DAR measurement using the present phase system [15]. Mobile phase B contained 10 mM monosodium phosphate and 8 V/V% IPA. Before adding the organic modifier, the pH of mobile phase B was set to 7.0 by titrating with 1 M NaOH solution. Gradients from 0 to 100% B were performed using a flow rate of 0.6 mL/min on a MAbPac HIC-10 (100  $\times$  4.6 mm, 5  $\mu$ m, 1000 Å) column, purchased from Thermo Fisher Scientific AG (Reinach, Switzerland). To obtain input data for retention modelling, gradient time was set either to  $t_{G,1}$  = 10 min and  $t_{G,2}$  = 30 min, and both linear and logarithmic gradients were performed. For studying the accuracy of retention time prediction, gradients of 20 min were run in both linear and logarithmic modes (0–100%B). To compare the selectivity distribution and elution window of the solutes, power function based gradients were also performed (see in Section 2.5.). Finally, logarithmic gradient has been optimized and gradient of 22 min were run with initial mobile phase composition of  $\varphi_i$  = 0.05 (5%B) and  $\varphi_i$  = 0.1 (10%B).

Column temperature was set to 25 °C. A sample volume equal to 3  $\mu$ L was injected using the partial loop injection mode. The FL detector was operated at 280 nm excitation and 360 nm emission wavelengths, at 2 Hz sampling rate.

### 2.4. Software

Calculations based on linear and multi-linear gradients and data transferring was achieved with DryLab 4 (Molnar Institute, Berlin) and Excel templates (MS Office). For the logarithmic gradient based retention models and selectivity mapping, PyLSS software (<https://github.com/gmrandazzo/PyLSS>) as an open-source software was used.

### 2.5. Apparatus and methodology

The Linear Solvent Strength (LSS) model is frequently applied in various modes of liquid chromatography to describe the relationship between the solute retention and experimental conditions (i.e. gradient slope or mobile phase composition) [21]. The dependence of the retention on the mobile phase salt concentration (ionic strength) determines the applicability of the LSS model for gradient elution in HIC [22]. It was experimentally shown by Szepeszy and Karger that the retention of some common proteins in HIC gradient mode follows the LSS model [23,24]. It has recently been reported that LSS retention model can be applied for the optimization of ADC species separation and retention time prediction were excellent for linear and for 2-segment multi-linear gradients [13,14].

Based on the LSS theory, in isocratic elution mode, a logarithmic retention factor ( $\ln(k)$ ) vs. mobile phase composition ( $\varphi$ ) function typically shows linear behavior and can be expressed as:

$$\ln k = \ln k_0 - S \cdot \varphi \quad (1)$$

where  $k$  is the retention factor ( $k = (t_r - t_0)/t_0$ ,  $t_r$  refers to the solute retention time and  $t_0$  refers to the column dead time),  $\varphi$  is the volume fraction of mobile phase “B” (containing no salt),  $S$  is a constant for a given compound at fixed experimental conditions (other than  $\varphi$ ), and  $k_0$  is the (extrapolated) value of  $k$  for  $\varphi = 0$  (i.e., the retention factor observed in pure mobile phase “A”, containing salt).

In HIC practice, an inverse salt gradient is applied to elute proteins from a mildly hydrophobic stationary phase. The retention (or retention time) of the solute can be calculated for any linear gradients based on the LSS theory, using the following equation:

$$t_r = \frac{t_G}{S \cdot \Delta\varphi} \ln \left( \frac{2.303 \cdot S \cdot \Delta\varphi \cdot t_0 \cdot k_0}{t_G} + 1 \right) + t_0 + t_d \quad (2)$$

where  $t_G$  is the gradient time (duration) and  $t_d$  is the system dwell time (gradient delay). Eq. (2) can be rearranged to give [25]:

$$\gamma = \frac{1}{S} \ln \Gamma + \frac{1}{S} \ln(S \cdot k_0) + \Gamma \quad (3)$$

where  $\gamma = 2.303 \cdot \Delta\phi \cdot t_r/t_G$  and  $\Gamma = 2.303 \cdot \Delta\phi \cdot t_0/t_G$ . After further rearrangement, the next formula can be obtained [25]:

$$\gamma - \Gamma = \frac{1}{S} \ln \Gamma + \frac{1}{S} \ln(S \cdot k_0) \quad (4)$$

This expression is particularly useful, since it yields  $1/S$  as the slope of the linear fit of  $\gamma - \Gamma$  versus  $\log \Gamma$ .

Finally, the  $\log k_0$  and  $S$  parameters of the HIC LSS model can be determined from two linear gradient runs obtained with different  $t_G$ . For extracting the LSS parameters, iteration has been performed on the basis of two linear gradients (DryLab 4 software was used).

It is known, that when separating homologous series of compounds, non-linear (concave) gradients (power-function based) can provide better selectivity than linear gradients [17–19]. It is due to the fact than in the case of homologues – when performing linear gradients – the selectivity decreases as the homologue number ( $n_h$ : number of interacting functional groups) increases. For homologues with low numbers of functional groups, one additional functional group increases drastically the strength of interaction between the solute and the stationary phase. While, for homologues possessing high number of functional groups, one additional functional group will increase the strength of their interaction only to a small extent. Therefore, the unequal peak spreading that is often observed in the chromatograms is due to the gradually decreasing molecular difference among the species possessing higher position in the series. As an example, the difference in hydrophobicity of DAR0 and DAR2 species of a cysteine conjugated ADC is significantly larger than of the DAR6 and DAR8 species. Fig. 1A shows the possible DAR species and positional isomers of cysteine conjugated ADC, while Fig. 1B illustrates the drug linker, spacer and cytotoxic agent.

For the above discussed reasons, a logarithmic gradient profile is proposed in this study to increase selectivity between high DAR species and decrease the “non-useful” elution space between the low DAR species. Logarithmic gradients were performed by approaching the logarithmic gradient shape with multilinear gradients. This way, the retention of solutes can be predicted for logarithmic-like gradient profiles on the basis of two linear scouting gradients. However, the LSS model can also be extended for logarithmic gradient profile. Then, performing two scouting logarithmic gradients – instead of linear ones – probably provides a more accurate and reliable retention time prediction and can offer benefits for method development. To derive the analytical solution for the logarithmic gradient profile, we must start to differentiate the definition of retention factor  $k$ , to get the fundamental gradient equation:

$$\int_0^{t_R} \frac{1}{t_0} \cdot \frac{1}{k(t)} \cdot dt = 1 \quad (5)$$

Where  $t_0$  is not varying with the solvent composition,  $k(t)$  is the retention factor as a function of time.

In a linear gradient, the mobile phase composition ( $\phi$ ) varies linearly with time ( $\phi = f(t)$ ), according to a linear relationship:

$$\phi(t) = \phi_i + \frac{(\phi_f - \phi_i)}{t_G} \cdot t \quad (6)$$

where  $t$  is the actual time of the gradient program,  $\phi_i$  and  $\phi_f$  are the initial and final mobile phase compositions, respectively. In our case, we decided to use a simple nonlinear concave shape in which

the solvent composition varies logarithmically with time. Thus, a relative scale  $\frac{\Delta t}{\min}$  must be defined to obtain the following equation:

$$\phi \frac{\Delta t}{\min} = f \left( \frac{\Delta t}{\min} \right) \equiv \phi_i + \frac{(\phi_f - \phi_i)}{\ln \left( \frac{t_G + 1}{\min} \right)} \cdot \ln \left( \frac{t + 1}{\min} \right) \quad (7)$$

where  $\frac{(\phi_f - \phi_i)}{\ln \left( \frac{t_G + 1}{\min} \right)}$  is the logarithmic gradient steepness, described as  $\alpha$ .

By combining the fundamental LSS relation (see Eq. (1)) in which the natural logarithm of the retention factor  $k$  varies linearly with the solvent strength composition, together with the logarithmic relation for the solvent composition, the following equation can be obtained:

$$\ln(k) = \ln(k_{0i}) - S \cdot \alpha \cdot \ln \left( \frac{t + 1}{\min} \right) \quad (8)$$

where  $k_{0i}$  is the retention factor observed when using the initial mobile phase composition,  $S$  is a molecular parameter and  $\alpha$  is the logarithmic gradient steepness. By substituting Eq. (8) into Eq. (5), integrating and solving the equation – considering also the dwell time –, an analytical solution can be obtained, able to estimate the retention time of solutes for any logarithmic gradient conditions:

$$t_R = (t_0 \cdot k_{0i} \cdot (S \cdot \alpha + 1)^{\frac{1}{S\alpha+1}}) - t_d - 1 \quad (9)$$

Through this equation and two simple logarithmic gradients, it was possible to estimate the  $\ln(k_0)$  and  $S$  parameters by iterative calculations and thus to predict the retention time for various logarithmic gradients (e.g. for various  $t_G$  and  $\phi_i$ ).

Thanks to the instrument control with Empower Pro 3 software, various shape “built-in” concave gradients were performed based on the following power-functions [18,19].

$$\phi(t) = \phi_i + (\phi_f - \phi_i) \left( \frac{t}{t_G} \right)^n \quad (10)$$

$$n = \frac{1}{2}; \frac{1}{3}; \frac{1}{4}; \frac{1}{5} \quad (11)$$

where  $n$  is the exponent of the power function. Exponent values of  $0 < n < 1$  give concave gradients. The four different concave gradients were run ( $t_G = 20$  min) to compare their selectivity and elution window vs. logarithmic gradient.

### 3. Results and discussion

#### 3.1. Expected retention distribution of ADC homologues in HIC

Homologous series are particularly useful for the investigation of retention mechanism in liquid chromatography and potentially attractive for the calibration of retention, because they allow studying the specific contribution to retention caused by a regular increase in the length or number of the functional groups [17,26]. A regular linear increase of the logarithmic retention factor with increasing number of carbon atoms in a homologous series has been reported for a number of homologous series in both RP and HIC systems [17,26,27]. This behavior is to be expected from the Martin rule of additivities of the molecular increments to retention and often called as the “homologue-rule”. It has also been reported that for some homologues - deviations from linear relationship of  $\log k - n_h$  can be observed in a wide range of conditions and semi-logarithmic or quadratic relationship could result in a better fit [17].

Based on two linear scouting gradients ( $t_G = 10$  and 30 min), the LSS parameters ( $k_0$  and  $S$ ) were obtained for DAR0, DAR1, DAR2, DAR3, DAR4, DAR6 and DAR8 species and retention factors ( $k$ ) for an isocratic separation at  $\phi = 0.8$  were calculated. As expected,

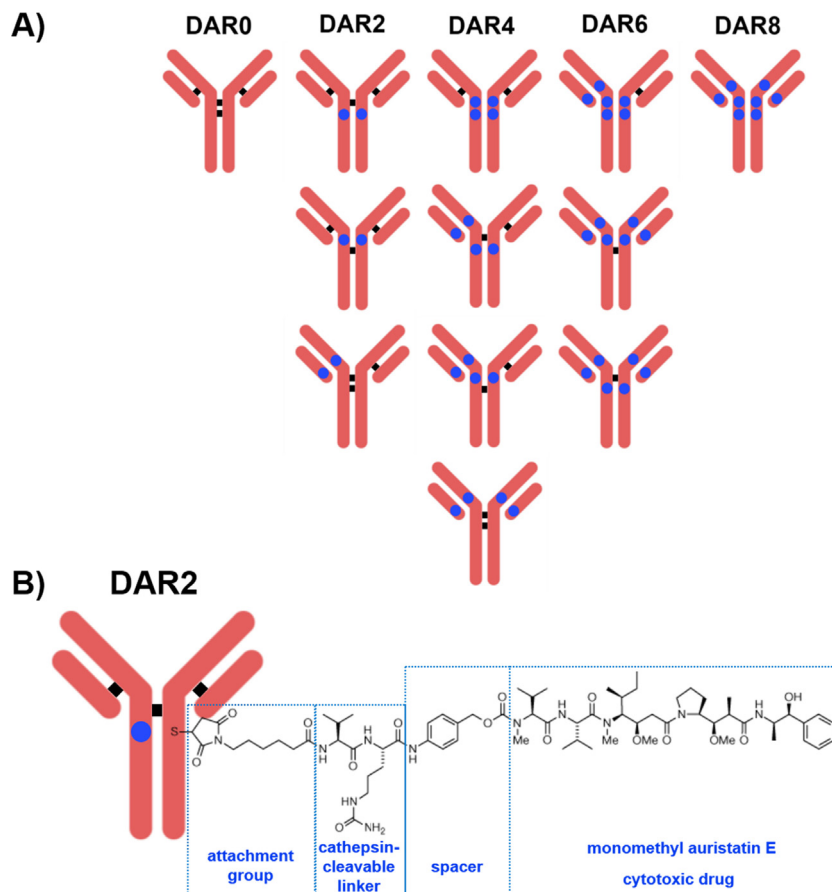


**Fig. 1.** Possible DAR species of a cysteine conjugated ADC (A) and structure of doubly loaded brentuximab-vedotin (B). Please note that odd DAR species may appear in real samples since they are degradation products of even DAR species.

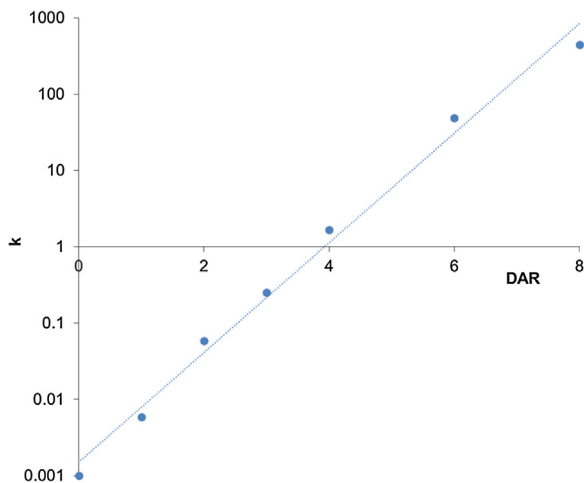


**Fig. 2.** Calculated retention factors for 80% B isocratic elution of DAR homologues with log-k scaling vs. number of functional groups (DARs).

when plotting the calculated retention factors in a logarithmic scale versus DAR number (or  $n_h$ ), a linear relationship was observed (Fig. 2). However, due to the large  $S$  values of macromolecules, isocratic separation is hardly feasible, moreover it would require very long analysis time. Therefore, calculations were done to study the distribution of peaks (as normalized apparent retention factors,  $k_{app}$ ) and the evolution of selectivity for various gradients including linear, power function based and logarithmic ones (for  $t_G = 20$  min and from  $\varphi_i = 0$  to  $\varphi_f = 1$ ).

Fig. 3 shows the normalized  $k_{app}$  values as a function of DAR number for various gradients. Since we were interested in selectivity and not in the absolute retention, the retention factors were normalized for the  $k_{app}$  range between DAR0 and DAR8. We considered the retention of DAR0 as 0% and as 100% for DAR8. This way, the retention distribution and selectivity are directly comparable. Curves have been fitted to better see the tendencies. The more linear the curve, the more equidistant the retention distribution is. In other words, when the fitted curve is close to a linear trend, then the selectivity becomes more constant between all the species. With a regular linear gradient, the fitted curve is quite steep in the range of low DARs (DAR0–DAR4) but it becomes flat for high DARs (DAR4–DAR8). It suggests that linear gradient provides high selectivity for low DARs but relatively poor selectivity for high DARs. In practice, the most critical peak pair to be separated in HIC is the DAR6–DAR8, and linear gradients can hardly separate these species. When using a power function based non-linear gradient with  $n > 1$  (convex gradient, see Eq. (10)), a similar tendency was observed as with linear gradients, but to a higher extent. Indeed, the selectivity further improves for low DARs (unnecessarily) and decreases for high DARs (not sufficient). In contrast, concave gradients ( $0 < n < 1$ ) clearly improve the selectivity between high DARs but also decrease selectivity for low DAR species. Those concave gradients with  $1/2 < n < 1/5$  are obviously more useful than linear gradient. A too low  $n$  values (e.g.  $n = 1/10$ ) provides insufficient selectivity for low DARs, but gives high selectivity for DAR6–DAR8 peak pair, that is typically the most challenging one with “common” linear gradients. As expected from the “homologue-rule”, a logarithmic gradient should provide the most equidistant retention distribution for the ADC DAR species. In agreement with this expect-

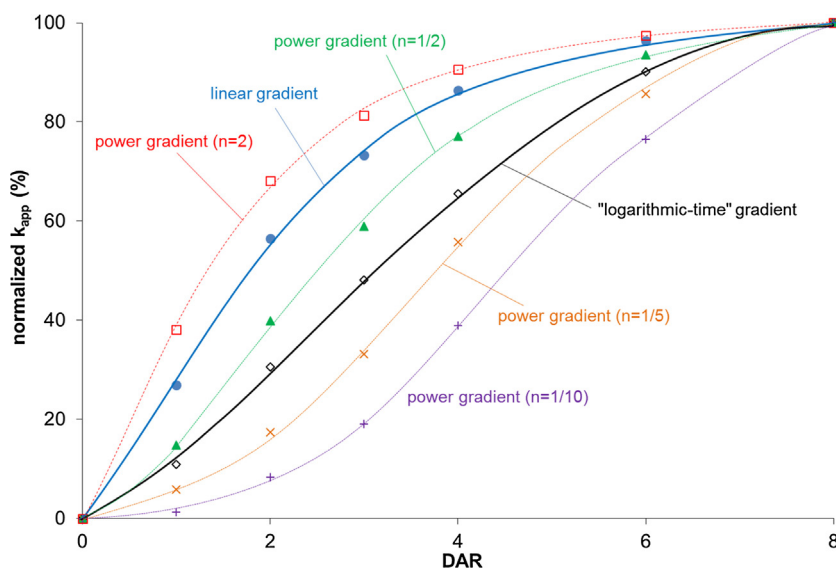


Fig. 3. Normalized  $k_{app}$  vs. DAR calculated for various gradient programs for optimizing selectivity.

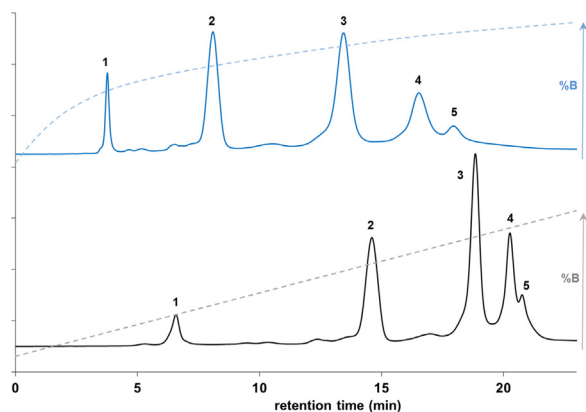


Fig. 4. Linear (black) vs. logarithmic (blue) gradient profiles and chromatograms of brentuximab-vedotin. Peaks: DAR0 (1), DAR2 (2), DAR4 (3), DAR6 (4) and DAR8 (6). Mobile phase A: 4 M NaCl with 10 mM phosphate buffer (pH = 7), mobile phase B: 10 mM phosphate buffer (pH = 7) with 8% IPA. Column: Thermo Fisher Scientific MAbPac HIC-10 (100 × 4.6 mm, 5  $\mu$ m, 1000 Å), T: 25 °C, gradient program: 0–100% B in 20 min, flow: 0.6 mL/min. (For interpretation of the references to colour in this figure legend, the reader is referred to the web version of this article.)

tation, the logarithmic gradient provided indeed the best overall selectivity. It leads to an appropriate selectivity for high DARs without ruining the separation of low DARs. As a conclusion, based on our calculations, a logarithmic gradient indeed offers the best overall separation of cysteine linked ADC DAR series in HIC.

### 3.2. Impact of gradient shape on selectivity and elution window

In Section 3.1, calculations based on two scouting linear gradients were discussed to estimate the selectivity of ADC DARs for various non-linear gradient conditions. In Section 3.2, experimentally observed results are discussed. Linear, logarithmic and power function based gradients were performed (with  $t_G = 20$  min and from  $\varphi_i = 0$  to  $\varphi_f = 1$ ).

Fig. 4 shows a comparison of the chromatographic profiles obtained with usual linear and logarithmic gradients for brentuximab-vedotin (commercial cysteine conjugated ADC). With the linear gradient (black chromatogram in Fig. 4), the selectivity continuously decreases between the consecutively eluted species. The separation was quite poor between peaks 4 and 5 (correspond-

ing to DAR6 and DAR8), while the peak spacing was unnecessarily large between peaks 1 and 2 (corresponding to DAR0 and DAR2). With the logarithmic gradient (blue chromatogram in Fig. 4), which was approached by a ten-segment multi-linear gradient (see Section 3.3), the separation of high DARs improved (close to baseline resolution was reached between DAR6 and DAR8), whereas the superfluously large distance between DAR0 and DAR2 decreased. Another important advantage of the logarithmic gradient against the linear one is its peak focusing effect for the DAR0 species. The peak is compressed because of changes of its trajectory while crossing the gradient within the column. During gradient elution, the rear part of the peak moves faster than its front part, because the mobile phase strength increases along the column [28]. This phenomenon is better known under the name of band compression. The steeper the gradient, the higher the band compression effect is [28]. Since the gradient steepness is higher at the beginning with the logarithmic vs. linear gradient profile, the DAR0 species was more focused and eluted as sharp peak. It is useful because the concentration of DAR0 is generally very low (the naked mAb is considered as an impurity of the ADC). By utilizing the peak focusing effect, the quantitation limit of DAR0 can thus be improved (Please note that for our experiments an old brentuximab-vedotin sample was used that contained relatively high amount of DAR0).

The concave power function based gradient profiles were compared on Fig. 5. As expected, they all provide better selectivity for high DARs than linear gradient and decreases the elution distance between low DAR species. Thus, power function based concave gradients have similar effect on the separation as logarithmic gradient, but to a different extent. As shown in Fig. 5, a power function gradient with exponent of  $n = 1/3$  gives appropriate chromatographic profile for separating DAR species of ADC. With the power function gradients – similarly to the logarithmic ones – the beneficial peak focusing for DAR0 was also observed. Another advantage of built-in power gradients is that elution window can easily be adjusted. As an example the power gradient with  $n = 1/2$  resulted in 2.5 times larger elution window than the gradient with  $n = 1/5$  (see Fig. 5).

### 3.3. Approaching logarithmic gradient with multi-linear ones

As expected and observed for ADC DAR homologous series, the logarithmic gradient program seems to be the most suitable. Table 1 shows the resulting selectivity and resolution values for

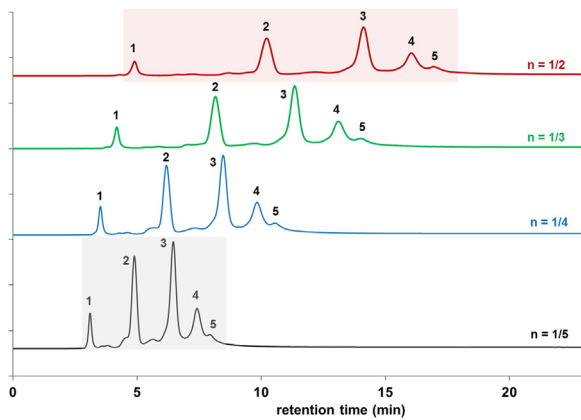


**Fig. 5.** Chromatograms obtained with built-in power shaped gradient programs of the chromatographic system.  $n = 1/5 - 1/2$  corresponds to curvature 2 – 5 in the gradient table of the Empower Pro 3 software. Mobile phase A: 4 M NaCl with 10 mM phosphate buffer (pH = 7), mobile phase B: 10 mM phosphate buffer (pH = 7) with 8% IPA. Column: Thermo Fisher Scientific MAbPac HIC-10 ( $100 \times 4.6$  mm,  $5 \mu\text{m}$ , 1000 Å), T: 25 °C, gradient program: 0–100% B in 20 min, flow: 0.6 mL/min. Peaks: DAR0 (1), DAR2 (2), DAR4 (3), DAR6 (4) and DAR8 (6) species of brentuximab-vedotin.

**Table 1**  
Selectivity ( $\alpha$ ) and resolution ( $R_s$ ) of DAR species using various gradient profiles with the same chromatographic conditions.

$\alpha$	$n = 1/5$	$n = 1/4$	$n = 1/3$	$n = 1/2$	logarithmic	linear
DAR 0–1	1.68	1.74	1.79	1.82	1.84	1.84
DAR 1–2	1.62	1.62	1.60	1.59	1.94	1.51
DAR 2–3	1.17	1.26	1.25	1.24	1.39	1.19
DAR 3–4	1.33	1.23	1.22	1.19	1.35	1.13
DAR 4–6	1.22	1.21	1.19	1.16	1.27	1.08
DAR 6–8	1.09	1.09	1.08	1.06	1.10	1.03
$R_s$	$n = 1/5$	$n = 1/4$	$n = 1/3$	$n = 1/2$	logarithmic	linear
DAR 0–1	1.73	2.14	2.39	2.43	1.72	2.97
DAR 1–2	2.23	2.56	2.68	2.69	2.62	3.01
DAR 2–3	1.68	1.69	1.83	1.91	1.82	2.00
DAR 3–4	1.77	1.77	1.97	1.96	2.13	1.89
DAR 4–6	1.89	2.04	2.19	2.24	2.71	2.04
DAR 6–8	0.70	0.74	0.71	0.59	0.87	0.27

DAR species when using various gradient profiles. Indeed, logarithmic gradient profile provided the best separation for high DAR species of D6 and D8, which are considered to be the critical peak pair. For other DAR species baseline resolution was observed. The only problem with this approach is that the logarithmic gradient program is not built in any chromatographic software. To implement this gradient curvature, one can approach the logarithmic

function with a multi-linear gradient. The higher the number of the multi-linear gradient segments, the more accurate the approaching to the logarithmic function is. Based on our experiments, a 10-segment multi-linear gradient – which approaches the logarithmic curvature – gives indeed an excellent separation (very close to a “real” logarithmic elution profile). Fig. 6 illustrates this gradient program and the chromatographic profile of brentuximab-vedotin. However, the drawback of this 10-segment multi-linear gradient is that it is time-consuming to write such a gradient program and therefore probably it would not be accepted in routine pharmaceutical laboratories. On the other hand, for routine use this has to be done once and the same method can be used for further analyses. From practical points of view the minimum number of multi-linear gradient segments required to maintain the quality of the separation and the “logarithmic-like” chromatographic profile was determined. After an optimization process, it was found that a multi-linear gradient with 4 segments was still appropriate, when setting the mobile phase composition at the 10, 30, 50 and 100% of  $t_G$ . Obviously, shorter segments were required at the beginning of the gradient (as the 10 and 30% segments of  $t_G$ ), since the steepness of logarithmic curvature changes more intensively. Fig. 7 shows an example of a 4-segment based multi-linear gradient. It can be seen that indeed a very similar separation was achieved as on Fig. 4, where a 10-segment based multi-linear gradient was applied. Even if the retention distribution of the DAR species was not exactly the same as with a “true” logarithmic gradient profile, the 4-segment based multi-linear gradient still provides better overall selectivity as any of the Empower’s built in concave gradient functions. In supplementary material 1, a 4- and a 10-segment based multi-linear gradient programs were provided for 20 min long gradient. These gradients are particularly useful for routine applications when operating  $100 \times 4.6$  min HIC columns (for other column dimensions, the gradient has to be geometrically transferred).

The benefit of approaching a logarithmic gradient program with a limited number of multi-linear segments (e.g. 4 segments) is that a very accurate retention time prediction is feasible on the basis of only two scouting linear gradients (common LSS modelling can be applied). An average error of less than 1.5% was observed for retention time prediction (using DryLab 4 software). Fig. 7 also shows a comparison of predicted and experimentally observed chromatograms. More details on retention time prediction accuracy are provided in Section 3.4.

### 3.4. Optimization and accuracy of retention time prediction

First, the appropriate phase system (column, mobile phase salt type and salt concentration) has to be found and the elution win-

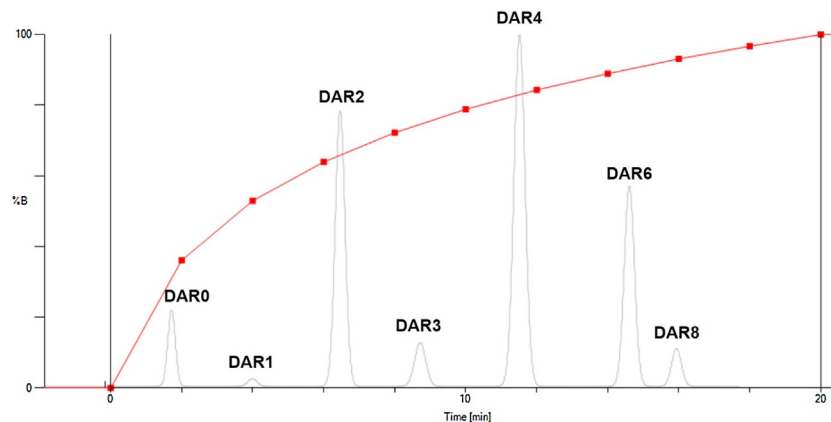


**Fig. 6.** Approximation of logarithmic gradient by a 10-segment multi-linear gradient based on LSS model and two scouting linear gradients.

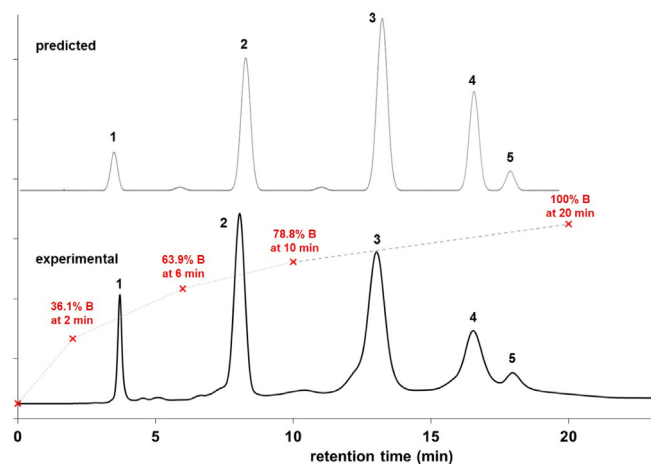


**Fig. 7.** Approximation of logarithmic gradient by a 4-segment multi-linear gradient and experimental verification. Mobile phase A: 4 M NaCl with 10 mM phosphate buffer (pH = 7), mobile phase B: 10 mM phosphate buffer (pH = 7) with 8% IPA. Column: Thermo Fisher Scientific MAbPac HIC-10 (100 × 4.6 mm, 5 μm, 1000 Å), T: 25 °C, gradient program: 0–100% B in 20 min, flow: 0.6 mL/min. Peaks: DAR0 (1), DAR2 (2), DAR4 (3), DAR6 (4) and DAR8 (6) species of brentuximab-vedotin.

dow has to be set to have sufficient retention for DAR0 and to elute the DAR8 species. This “method screening approach” and procedure for ADCs has recently been reported by our group [14]. For the correct determination of average DAR, it has been shown that organic modifiers should be added to mobile phase B (5–20%, depending on the salt system and recovery of high DAR species) [15]. Here, we do not discuss this method screening process in details, as it is out of the scope of the present study. Based on preliminary results, the most efficient commercially available column, an appropriate phase system and conditions have been selected for the gradient optimization (see conditions in Section 2.3).

To further optimize the HIC separation of ADC DAR species, two possibilities could exist: (1) The first option is to run two linear scouting gradients and then calculating (optimizing) the retention and selectivity between all studied analytes, for any linear or multi-linear gradients (including logarithmic-like too), based on a common LSS model. (2) The second possibility is to already run two logarithmic-like scouting gradients and then optimize the separation on the basis of the extended LSS model for logarithmic gradient profile (derived in Section 2.5). For both approaches, the method parameters to be optimized are: (i) the initial mobile phase composition, (ii) the final mobile phase composition and (3) the gradient time. The benefit of the first approach is that any gradient program (approached by multi-linear gradients) can be optimized on the basis of linear scouting gradients and commercially available software can be used for optimization (e.g. DryLab). The advantage of the second approach – and its novelty – is that the theoretically expected best selectivity can be reached already during the scouting gradients and it may happen that there will be no further need for optimization (since a logarithmic gradient should already provide the best separation of homologous series if the initial and final mobile phase composition have been properly set). An example is shown in Fig. 8 for the optimization based on two logarithmic-like scouting gradients. The 10 and 30 min long scouting gradients already resulted in appropriate separations, however by fine tuning the initial mobile phase composition ( $\varphi_i = 0.1$ ) and gradient time ( $t_G = 22$  min), a slightly better separation could be achieved (Fig. 8). This separation is probably one of the best separations that can be achieved for this particular ADC – on this given stationary phase and column dimension –, when considering both selectivity and analysis time.

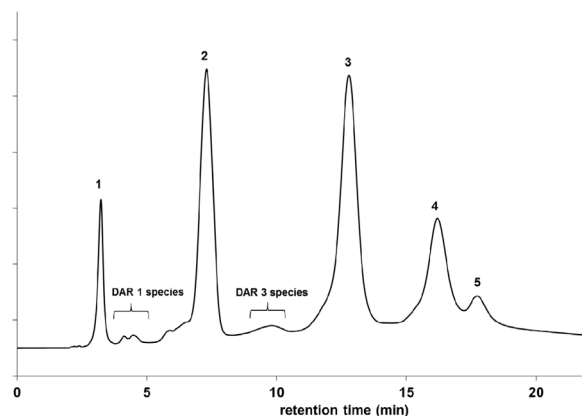


**Fig. 8.** Optimized logarithmic-like gradient. Mobile phase A: 4 M NaCl with 10 mM phosphate buffer (pH = 7), mobile phase B: 10 mM phosphate buffer (pH = 7) with 8% IPA. Column: Thermo Fisher Scientific MAbPac HIC-10 (100 × 4.6 mm, 5 μm, 1000 Å), T: 25 °C, gradient program: 10–100% B in 22 min (10-segment multi-linear gradient), flow: 0.6 mL/min. Peaks: DAR0 (1), DAR2 (2), DAR4 (3), DAR6 (4) and DAR8 (6) species of brentuximab-vedotin. DAR1 and DAR3 species are degradation products of even DAR species [29,30].

**Table 2**

Accuracy of retention time predictions based on two scouting linear gradients ( $t_{G1} = 10$  min,  $t_{G2} = 30$  min, 0 – 100%B).

Prediction for 20 min long linear gradient (0–100% B)				
peaks	retention times			
	experimental	predicted	difference	abs. error%
DAR 0	6.53	6.63	–0.10	–1.5
DAR 1	10.28	10.44	–0.16	–1.5
DAR 2	14.52	14.64	–0.12	–0.8
DAR 3	16.92	17.01	–0.09	–0.5
DAR 4	18.77	18.86	–0.09	–0.5
DAR 6	20.20	20.29	–0.09	–0.4
DAR 8	20.70	20.80	–0.10	–0.5
average:				–0.8
Prediction for 20 min long logarithmic-like gradient (0–100% B) performed with 10-segment multi-linear gradient				
peaks	retention times			
	experimental	predicted	difference	abs. error%
DAR 0	3.77	3.65	0.12	3.3
DAR 1	5.19	5.12	0.07	1.4
DAR 2	8.11	8.04	0.07	0.9
DAR 3	10.59	10.56	0.03	0.3
DAR 4	13.46	13.4	0.06	0.4
DAR 6	16.55	16.49	0.06	0.4
DAR 8	17.96	17.82	0.14	0.8
average:				1.1
Prediction for 22 min long logarithmic-like gradient (10–100% B) performed with 10-segment multi-linear gradient				
peaks	retention times			
	experimental	predicted	difference	abs. error%
DAR 0	3.23	3.18	0.05	1.5
DAR 1	4.48	4.58	–0.10	–2.2
DAR 2	7.30	7.51	–0.21	–2.8
DAR 3	9.80	10.02	–0.22	–2.2
DAR 4	12.79	13.03	–0.24	–1.8
DAR 6	16.19	16.76	–0.57	–3.4
DAR 8	17.73	18.39	–0.66	–3.6
average:				–2.1

Another interesting aspect is the accuracy of the retention models. The prediction errors were determined for various gradient conditions, using both linear and logarithmic models. Table 2 shows

**Table 3**

Accuracy of retention time prediction based on two logarithmic-like scouting gradient runs ( $t_{G1} = 10$  min,  $t_{G2} = 30$  min, 0–100%B, logarithmic gradient was approached by 10-segment multi-linear gradient).

Prediction for 20 min long logarithmic-like gradient (0–100% B) performed with 10-segment multi-linear gradient				
peaks	retention times			
	experimental	predicted	difference	abs. error%
DAR 0	3.77	3.82	0.05	1.3
DAR 1	5.19	5.18	−0.01	0.2
DAR 2	8.11	8.12	0.01	0.1
DAR 3	10.59	10.61	0.02	0.2
DAR 4	13.46	13.50	0.04	0.3
DAR 6	16.55	16.59	0.04	0.2
DAR 8	17.96	17.96	0.00	0.0
average:				0.3

Prediction for 22 min long logarithmic-like gradient (10–100% B) performed with 10-segment multi-linear gradient				
peaks	retention times			
	experimental	predicted	difference	abs. error%
DAR 0	2.99	3.17	0.18	6.0
DAR 1	4.36	4.53	0.17	3.9
DAR 2	7.16	7.44	0.28	4.0
DAR 3	9.80	9.88	0.08	0.8
DAR 4	12.75	12.88	0.13	1.0
DAR 6	15.99	16.34	0.35	2.1
DAR 8	17.63	17.81	0.18	1.0
average:				2.7

Prediction for 22 min long logarithmic-like gradient (5–100% B) performed with 15-segment multi-linear gradient				
peaks	retention times			
	experimental	predicted	difference	abs. error%
DAR 0	3.21	3.33	0.12	3.7
DAR 1	4.66	4.80	0.14	2.9
DAR 2	7.56	7.82	0.26	3.5
DAR 3	10.00	10.30	0.30	3.0
DAR 4	13.13	13.30	0.17	1.3
DAR 6	16.37	16.70	0.33	2.0
DAR 8	18.01	18.13	0.12	0.7
average:				2.4

three cases, for which the prediction was based on two linear scouting gradients. In the first case, only the gradient time was changed. Based on the 10 and 30 min long linear gradients, retention times were predicted for a 20 min long linear gradient. The experimental and predicted retention times were in excellent agreement. Only a −0.8% average error was found. In the second case, retention times were predicted for a logarithmic-like 10-segment based multi-linear gradient ( $t_G = 20$  min). Again, very good accuracy was found as the average error in retention time prediction was about 1.1%. In the third case, a logarithmic-like gradient was again simulated, but the initial mobile phase composition was changed to 10% B and the gradient time to 22 min. As expected, the retention time prediction error increased, but remained still acceptable (−2.1% average error). **To conclude, performing linear scouting gradients enables to accurately predict retention times for multi-linear gradients (logarithmic-like) by using commercial software package (DryLab).**

Table 3 shows three other cases for which the retention time prediction was based on logarithmic scouting gradients. For this purpose, our proposed logarithmic retention model was applied. In the first case, only the gradient time was changed. Based on 10 and 30 min long logarithmic-like gradients, retention times were predicted for a 20 min long logarithmic gradient. As expected, a very low error was observed (0.3% average error). The second case

represents the accuracy when the initial mobile phase composition was also changed (10%B). In these conditions, the average error was 2.7%, which can still be considered as an accurate prediction. The difference between experimental and predicted retention times can probably be explained by the fact that the model was based on “true” logarithmic function, while the scouting gradients were “just” logarithmic-like gradients, since “true” logarithmic gradient cannot be performed. To improve the retention model accuracy, the number of multi-linear segments was increased. The third example shows the prediction accuracy when the logarithmic gradient was approached by a 15-segment multi-linear gradient and when starting the separation from 5%B (gradient program is listed in Supplementary material 1). Here, the observed average error in retention time prediction was reduced to 2.4% and the accuracy improved significantly for the early eluting species. To summarize, our proposed logarithmic gradient retention model offers reliable retention time prediction and a useful tool for optimizing the chromatographic separation of homologous series.

Mapping the selectivity can be a valuable tool to find out the optimal conditions. In commercial software package (DryLab), the so-called resolution map is generally used to determine the most appropriate conditions, but it requires the correct setting of peak widths. With logarithmic gradients, the calculation of peak widths becomes challenging, due to the continuously changing band compressing effects (see Section 3.2). Prediction of peak widths is further complicated due to the heterogeneity of the DAR species. Therefore, we decided to monitor the change of selectivity (rather than resolution) as a function of gradient time (logarithmic profile) and initial mobile phase composition as method variables. Based on the retention model derived in this study, the selectivity ( $k_2/k_1$ ) was determined for all peak pairs. To map the selectivity, the “critical selectivity” was considered as the smallest selectivity (worst-case) among all selectivity values under a given condition. Then, this critical selectivity was calculated for various conditions and mapped as 2D contour plot with  $\varphi_i$  and  $t_G$  as variables. Fig. 9 shows the obtained selectivity map. As can be seen, the longer the gradient time, the higher the selectivity. On the other hand, the initial mobile phase composition had no significant effect on the critical selectivity. This behavior was expected since the logarithmic gradient profile should already provide the highest selectivity for the critical peak pairs. However, by adjusting the initial mobile phase composition, more equidistant peak (retention) distribution can be attained. For an initial composition higher than 10%B, the retention of the first peak (DAR0) was not sufficient.

Finally, the time spent for method development has also to be mentioned. By using the most common HIC column dimension (100 × 4.6 mm) and performing  $t_{G1} = 10$  min and  $t_{G2} = 30$  min scouting gradients (linear or logarithmic), the time required for the optimization becomes (10 + 30 min) × number of samples. Then the computer assisted method optimization takes maximum a few hours (including the input of retention data to build the model). In total – generally – the time spent for method development requires less than one working day.

#### 4. Conclusion

In this study, non-linear gradients were employed in HIC to improve the analytical characterization of ADCs. The evolution of selectivities between the different DAR species of a commercial ADC, namely brentuximab Vedotin were investigated for various gradient profiles, including linear, power function based and logarithmic ones. Because it is currently not possible to perform a logarithmic gradient with current LC systems, the logarithmic gradient shape was approached with multi-linear ones (four-segment multi-linear was found to be well adapted for routine application

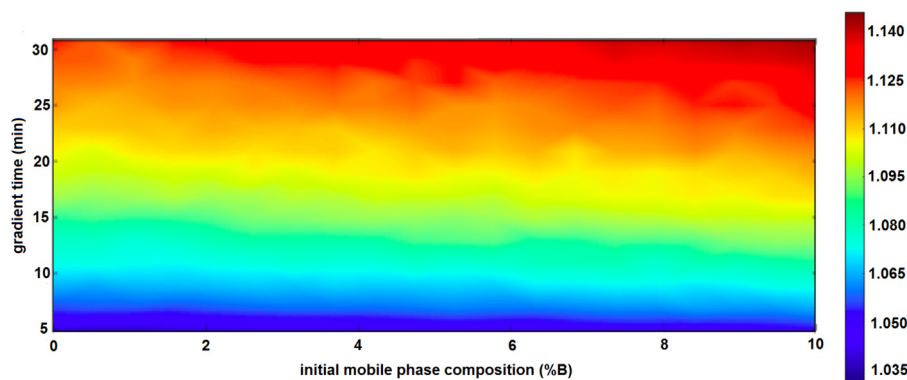


**Fig. 9.** Selectivity map based on logarithmic gradients. The critical selectivity was plotted as a function of the initial mobile phase composition ( $\varphi$ , or %B) and gradient time ( $t_G$  of logarithmic gradient profile). Red colors indicate high selectivity, while blue colors indicate low selectivity. (For interpretation of the references to colour in this figure legend, the reader is referred to the web version of this article.)

and remains easy to implement). As shown in this work, the logarithmic gradient provides better selectivity for high DARs than linear gradient and decreases the elution distance between low DAR species (in other words, it provides the most equidistant retention distribution for the ADC DAR species and offers the best overall separation of cysteine linked ADC in HIC). Another important advantage of the logarithmic gradient against the linear one, is its peak focusing effect for the DAR0 species. This is particularly useful because the concentration of DAR0 is often low (the naked mAb is considered as an impurity of ADC). By utilizing the peak focusing effect, the quantitation limit of DAR0 can thus be improved.

Then, two different approaches were implemented to model the logarithmic behavior of DAR species of ADC in HIC. First, the best logarithmic gradient profile was selected from the linear solvent strength theory (LSS), using only two scouting linear gradients and the predictions were carried out with a chromatographic modelling software (Drylab). The prediction accuracy was excellent and the errors for various gradient times and initial compositions were comprised between 0.8 and 2.1%, in average. In a second instance, the LSS model was extended to logarithmic gradient profile and a new solution was derived. Then, retention time predictions were possible based on two logarithmic scouting gradients. With this second approach, the prediction accuracy was again excellent and the average errors ranged from 0.3 to 2.7%.

## Acknowledgments

This study is dedicated to the memory of professor Jenő Fekete by Balázs Bobály and Szabolcs Fekete.

Davy Guillarme wishes to thank the Swiss National Science Foundation for support through a fellowship to Szabolcs Fekete (31003A\_159494).

The authors also wish to thank Dr Alain Beck and Olivier Colas (Center of Immunology Pierre Fabre in Saint-Julien en Genevois, France) for providing the Brentuximab Vedotin sample used in this study.

## Appendix A. Supplementary data

Supplementary data associated with this article can be found, in the online version, at <http://dx.doi.org/10.1016/j.chroma.2016.12.047>.

## References

- [1] A. Mullard, Maturing antibody-drug conjugate pipeline hits 30, *Nat. Rev. Drug Discov.* 12 (2013) 329–332.
- [2] S. Rostami, I. Qazi, R. Sikorski, The clinical landscape of antibody-drug conjugates, *ADC Review* <http://adcreview.com/articles/doi-10-14229/jadc-2014-8-1-001/> (Accessed 29 June 2016).
- [3] A. Beck, J.M. Reichert, Antibody-drug conjugates – present and future, *mAbs* 6 (2014) 15–17.
- [4] A. Wakankar, Y. Chen, Y. Gokarn, F.S. Jacobson, Analytical methods for physicochemical characterization of antibody drug conjugates, *mAbs* 3 (2011) 161–172.
- [5] F. Debaene, A. Boeuf, E. Wagner-Rousset, O. Colas, D. Ayoub, N. Corvaia, A. Van Dorsselaer, A. Beck, S. Cianferani, Innovative native MS methodologies for antibody drug conjugate characterization: high resolution native MS and IM-MS for average DAR and DAR distribution assessment, *Anal. Chem.* 86 (2014) 10674–10683.
- [6] E. Wagner-Rousset, M.-C. Janin-Bussat, O. Colas, M. Excoffier, D. Ayoub, J.-F. Haeuw, I. Rilatt, M. Perez, N. Corvaia, A. Beck, Antibody-drug conjugate model fast characterization by LC-MS following IdeS proteolytic digestion, *mAbs* 6 (2014) 173–184.
- [7] N. Said, R. Gahoual, L. Kuhn, A. Beck, Y.-N. François, Structural characterization of antibody drug conjugate by a combination of intact, middle-up and bottom-up techniques using sheathless capillary electrophoresis – tandem mass spectrometry as nanoESI infusion platform and separation method, *Anal. Chim. Acta* 918 (2016) 50–59.
- [8] A. Beck, G. Terral, F. Debaene, E. Wagner-Rousset, J. Marcoux, M.-C. Janin-Bussat, O. Colas, A. Van Dorsselaer, S. Cianferani, Cutting-edge mass spectrometry methods for the multi-level structural characterization of antibody-drug conjugates, *Expert Rev. Proteomics* 13 (2016) 157–183.
- [9] B. Wiggins, L. Liu-Shin, H. Yamaguchi, G. Ratnaswamy, Characterization of cysteine-linked conjugation profiles of immunoglobulin G1 and immunoglobulin G2 antibody-drug conjugates, *J. Pharm. Biomed. Anal.* 104 (2015) 1362–1372.
- [10] D. Firth, L. Bell, M. Squires, S. Estdale, C. McKee, A rapid approach for characterization of thiol-conjugated antibody-drug conjugates and calculation of drug-antibody ratio by liquid chromatography mass spectrometry, *Anal. Biochem.* 485 (2015) 34–42.
- [11] S. Fekete, J.-L. Veuthey, A. Beck, D. Guillarme, Hydrophobic interaction chromatography for the characterization of monoclonal antibodies and related products, *J. Pharm. Biomed. Anal.* 130 (2016) 3–18.
- [12] M. Haverick, S. Mengisen, M. Shameem, A. Ambrogelly, Separation of mAbs molecular variants by analytical hydrophobic interaction chromatography HPLC: overview and applications, *mAbs* 6 (2014) 852–858.
- [13] M. Rodríguez-Aller, D. Guillarme, A. Beck, S. Fekete, Practical method development for the separation of monoclonal antibodies and antibody-drug-conjugate species in hydrophobic interaction chromatography, part 1: optimization of the mobile phase, *J. Pharm. Biomed. Anal.* 118 (2016) 393–403.
- [14] A. Cusumano, D. Guillarme, A. Beck, S. Fekete, Practical method development for the separation of monoclonal antibodies and antibody-drug-conjugate species in hydrophobic interaction chromatography, part 2: Optimization of the phase system, *J. Pharm. Biomed. Anal.* 121 (2016) 161–173.
- [15] B. Bobály, A. Beck, J.-L. Veuthey, D. Guillarme, S. Fekete, Impact of organic modifier and temperature on protein denaturation in hydrophobic interaction chromatography, *J. Pharm. Biomed. Anal.* 131 (2016) 124–132.
- [16] T. Chen, Y. Chen, C. Stella, C.D. Medley, J.A. Gruenhagen, Antibody-drug conjugate characterization by chromatographic and electrophoretic techniques, *J. Chromatogr. B* 1032 (2016) 39–50.
- [17] P. Jandera, Simultaneous optimisation of gradient time, gradient shape and initial composition of the mobile phase in the high-performance liquid chromatography of homologous and oligomeric series, *J. Chromatogr. A* 845 (1999) 133–144.
- [18] V.S. Joshi, V. Kumar, A.S. Rathore, Role of organic modifier and gradient shape in RP-HPLC separation: analysis of GCSF variants, *J. Chromatogr. Sci.* 53 (2015) 417–423.

- [19] V. Joshi, V. Kumar, A.S. Rathore, Rapid analysis of charge variants of monoclonal antibodies using non-linear salt gradient in cation-exchange high performance liquid chromatography, *J. Chromatogr. A* 1406 (2015) 175–185.
- [20] L. Moruz, P. Pichler, T. Stranzl, K. Mechtler, L. Käll, Optimized nonlinear gradients for reversed-phase liquid chromatography in shotgun proteomics, *Anal. Chem.* 85 (2013) 7777–7785.
- [21] L.R. Snyder, J.W. Dolan, High-Performance Gradient Elution: The Practical Application of The Linear-Solvent-Strength Model, John Wiley & Sons, Inc, Hoboken, New Jersey, USA, 2007.
- [22] L.R. Snyder, J.J. Kirkland, J.L. Glajch, Practical HPLC Method Development, second ed., John Wiley & Sons Inc., 1997.
- [23] N.T. Miller, B.L. Karger, High-performance hydrophobic-interaction chromatography on ether-bonded phases: chromatographic characteristics and gradient optimization, *J. Chromatogr.* 326 (1985) 45–61.
- [24] G. Rippel, Á. Bede, L. Szepeszy, Systematic method development in hydrophobic interaction chromatography I. Characterization of the phase system and modelling retention, *J. Chromatogr. A* 697 (1995) 17–29.
- [25] J.C. Ford, J. Ko, Comparison of methods for extracting linear solvent strength gradient parameters from gradient chromatographic data, *J. Chromatogr. A* 727 (1996) 1–11.
- [26] Y. Wei, C. Yao, J. Zhao, X. Geng, Influences of the mobile phase composition and temperature on the retention behavior of aromatic alcohol homologues in hydrophobic interaction chromatography, *Chromatographia* 55 (2002) 659–665.
- [27] E. Peris-Garcia, M.T. Ubeda-Torres, M.J. Ruiz-Angel, M.C. Garcia-Alvarez-Coque, Effect of sodium dodecyl sulphate and Brij-35 on the analysis of sulphonamides in physiological samples using direct injection and acetonitrile gradients, *Anal. Methods* 8 (2016) 3941–3952.
- [28] H. Poppe, J. Paanakker, J. Bronckhorst, Peak width in solvent-programmed chromatography: I. General description of peak broadening in solvent-programmed elution, *J. Chromatogr.* 204 (1981) 77–84.
- [29] M. Sarrut, A. Corgier, S. Fekete, D. Guillarme, D. Lascoux, M.-C. Janin-Bussat, A. Beck, S. Heinisch, Analysis of antibody-drug conjugates by comprehensive on-line two-dimensional hydrophobic interaction chromatography x reversed phase liquid chromatography hyphenated to high resolution mass spectrometry. I-Optimization of separation conditions, *J. Chromatogr. B* 1032 (2016) 103–111.
- [30] M. Sarrut, S. Fekete, M.-C. Janin-Bussat, O. Colas, D. Guillarme, A. Beck, S. Heinisch, Analysis of antibody-drug conjugates by comprehensive on-line two-dimensional hydrophobic interaction chromatography x reversed phase liquid chromatography hyphenated to high resolution mass spectrometry. II-Identification of sub-units for the characterization of even and odd load drug species, *J. Chromatogr. B* 1032 (2016) 91–102.